Mechanical properties and microstructures of a magnesium alloy gas tungsten arc welded with a cadmium chloride flux

Z.D. Zhang, L.M. Liu, Y. Shen, L. Wang*

State Key Laboratory of Material Surface Modification by Laser, Ion, and Beams, School of Materials Science and Engineering, Dalian University of Technology, Dalian 116024, PR China

ARTICLE DATA

Article history:
Received 17 August 2006
Accepted 23 October 2006

Keywords:
Mechanical
Activating flux
Gas tungsten arc weld
Magnesium alloy

ABSTRACT

Gas tungsten arc (GTA) welds were prepared on 5-mm thick plates of wrought magnesium AZ31B alloy, using an activated flux. The microstructural characteristics of the weld joint were investigated using optical and scanning microscopy, and the fusion zone microstructure was compared with that of the base metal. The elemental distribution was also investigated by electron probe microanalysis (EPMA). Mechanical properties were determined by standard tensile tests on small-scale specimens. The as-welded fusion zone prepared using a $CdCl_2$ flux exhibited a larger grain size than that prepared without flux; the microstructure consisted of matrix α-Mg, eutectic α-Mg and β-$Al_{12}Mg_{17}$. The HAZ was observed to be slightly wider for the weld prepared with a $CdCl_2$ flux compared to that prepared without flux; thus the tensile strength was lower for the flux-prepared weld. The fact that neither Cd nor Cl was detected in the weld seam by EPMA indicates that the $CdCl_2$ flux has a small effect on convection in the weld pool.

1. Introduction

Magnesium and its alloys are considered to be among the most promising material categories for the 21st century [1]. Having densities 36% less than Al and 78% less than steel, Mg alloys have excellent strength/weight ratios [2,3]. In addition to their intrinsic characteristics of low density and high specific strength and stiffness, their high recyclability is attractive in reducing environmental burdens. Research activity on the welding of Mg alloys has been published in recent years [4–10]. Various fusion welding processes, principally tungsten inert gas [TIG, referred to here as gas tungsten arc (GTA)]) and laser and electron beam welding, even laser-GTA hybrid welding, were employed in these investigations; both cast and wrought Mg alloys were evaluated. The GTA welding of Mg alloy with an activating flux has been carried out by several investigators [11–14]. This technique was invented in the 1960s by researchers at the Paton Electric Welding Institute in the Ukraine [15,16]. When using an activating flux, a thin layer of the flux is deposited on the surface of the joint before welding, using a brush or a dispenser such as a spray. Using activating fluxes for steels, increases of up to 300% in penetration capability have been realized compared with the conventional GTA welding process. Since microstructures in the weld determine the properties of the joints and are important areas of interest for Mg alloy welding research, the present paper focuses on

Table 1 – Standard welding conditions used for this program

Power supply	Electrode	Shielding gas	Welding current	Welding speed	Electrode gap
Alternate current	W(2% ThO_2), 2.4 mm	Ar, 10 L min-1	100A	200 mm/min	1 mm

* *Corresponding author*. Tel.: +86 411 84707817.
E-mail address: liulm@dlut.edu.cn (L.M. Liu).

1044-5803/$ – see front matter
doi:10.1016/j.matchar.2006.10.012

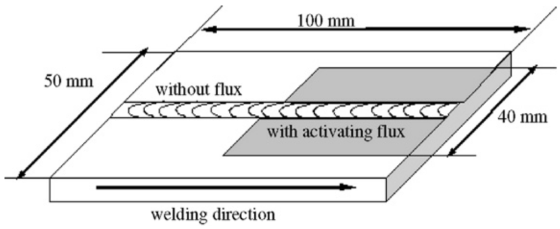

Fig. 1 – Schematic representation of the specimen used in the ACTIG welding of Mg alloy.

microstructural characterization and mechanical properties of the weld joint. The objective of the present paper is to report the results of comparative evaluation for GTA welded microstructures in a Mg alloy prepared with and without flux, and to provide an in-depth understanding of the weldability with the activated flux GTA weld process. In the previous series of experiments, the use of a cadmium chloride ($CdCl_2$) flux has the most pronounced effect on the increased weld penetration of welded magnesium alloys. In this paper, a cadmium chloride flux was selected as the flux ingredient to investigate the specific influence of the flux on weld penetration, microstructural characterization and mechanical properties of the weld joint.

2. Experimental

AZ31B magnesium alloy wrought plates, with the average composition of 3.10%Al, 0.65%Zn, >0.20%Mn, <0.10%Si, <0.03% Fe, <0.10%Cu, <0.005%Ni, <0.04%Ca, balance Mg, were selected for the welding experiments. The plates were machined into 100×50×5 mm rectangular plates to serve as the weld blanks. AC-GTAW bead-on-plate welds were made with an automatic control system in which the test piece was moved at a constant speed. The standard welding conditions used for these welds are listed in Table 1. The surfaces of the plates were chemically cleaned with acetone before welding to eliminate surface contamination. A single $CdCl_2$ flux was used to examine the mechanical properties and microstructure of the fluxed GTA weld. The flux was applied in powder form. The flux powder was mixed with acetone and applied with a brush to half of the top surface of a test piece (see Fig. 1).

After welding, the weld seam surface was photographed, and weld cross-sections were prepared using standard procedures including grinding, polishing, and etching. Transverse and longitudinal cross-sections macrographs were examined, and the penetration was measured. The microstructure of the weld joint was characterized by optical microscopy and scanning electron microscopy (SEM). The elemental distribution in the weld fusion zone was determined with energy dispersive spectroscopy (EDS) and electron probe microanalysis (EPMA). X-ray diffraction (XRD) analysis was used to identify phases in the weld fusion zone. In addition, the microhardness was measured to identify softening or hardening effects within the weld fusion zone and the HAZ.

In order to avoid the influence of the base metal (the weld joint is a partial penetration bead), only those parts of the joint which had been melted were machined into tensile specimens, in the form of a gauge section 15 mm long and 4 mm wide, as illustrated in Fig. 2. This enabled preparation of at least three specimens from each welded plate. Four types of tensile test specimens were machined from the joint: (i) base material in the rolling or parallel direction (H specimen); (ii) base material in the transverse or vertical direction (V specimen); (iii) transverse specimens containing the weld in the center of the gauge length with and without flux (T specimen); and (iv) longitudinal specimens machined along the weld metal with and without flux (L specimen). First, the upper surface was minimally machined in order to achieve a smooth surface. Then, the plate was machined from the other side to the thickness as the tensile test specimen (1–2 mm). Each data point reported below represents an average for least two to three specimens, which were tested to fracture in a hydraulic tensile-machine.

3. Result and Discussion

3.1. *Weld Seam Morphology*

Fig. 3 shows optical macrographs cross-sections, the longitudinal cross-sections and weld seam surfaces of welds made with and without the $CdCl_2$ flux at the standard welding condition. The increased weld penetration and more lustrous surface of welding with the $CdCl_2$ flux can be seen. The weld penetration (D) and weld depth/width (D/W) ratio with the flux was obviously higher than that of the welds prepared without the flux.

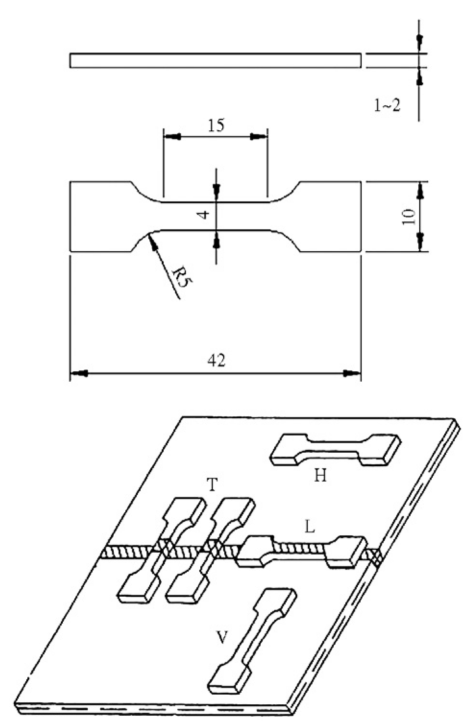

Fig. 2 – Schematic drawing of the three different tensile test specimens.

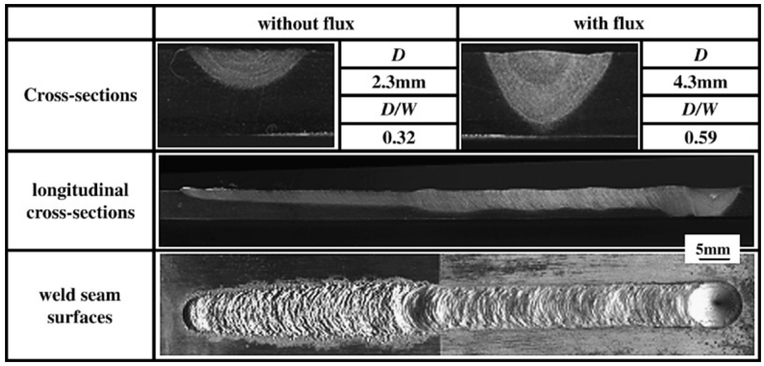

Fig. 3 – The cross-sections, longitudinal cross-sections and weld seam surfaces of welds.

3.2. *Microstructural Measurement*

The typical overall optical microstructure of the GTA welded Mg-AZ31B alloy with and without $CdCl_2$ flux is shown in Fig. 4. The HAZ and the weld seam are indicated. The as-welded fusion zone without flux (Fig. 4a) and with the $CdCl_2$ flux (Fig. 4b) all exhibited dendritic structure in the weld interior. Welds were found to be free from HAZ microfissuring both with and without the use of the flux (Fig. 4c, d). In a previous study, the arc voltage was found to be higher when the $CdCl_2$ flux is used in GTA welding of Mg-AZ31B alloy [12,14]. The heat input increases when the $CdCl_2$ flux is used under for the same welding speed and current used for conventional GTA welding. The HAZ was observed to be slightly wider with the $CdCl_2$ flux than for GTA welds prepared without flux; this is due to the increased heat input.

Optical micrographs, illustrating the crystal grain size of base metal, the weld seam and the HAZ, is shown in Fig. 5. The as-welded fusion zone prepared without the use of flux exhibited a finer grain size – about 20 μm – compared to the approximately 30 μm grain size for the flux-welded specimen, Fig. 5a, b. Fig. 5c shows the microstructure of the base metal. It is a typical wrought structure, with non-uniform grain size. During the welding process, the grain size in the HAZ grows. The microstructures in the HAZ of the welds prepared with and without the use of the flux are similar (Fig. 5 d,e). The HAZ structures are also non-uniform, with grain sizes varying from about 10 μm to 60 μm.

Fig. 6 presents secondary electron images of the weld fusion zone prepared with a flux. A number of white dots and black pits are visible inside the grain and occasionally at grain boundaries. According to the Mg–Al binary phase diagram, the

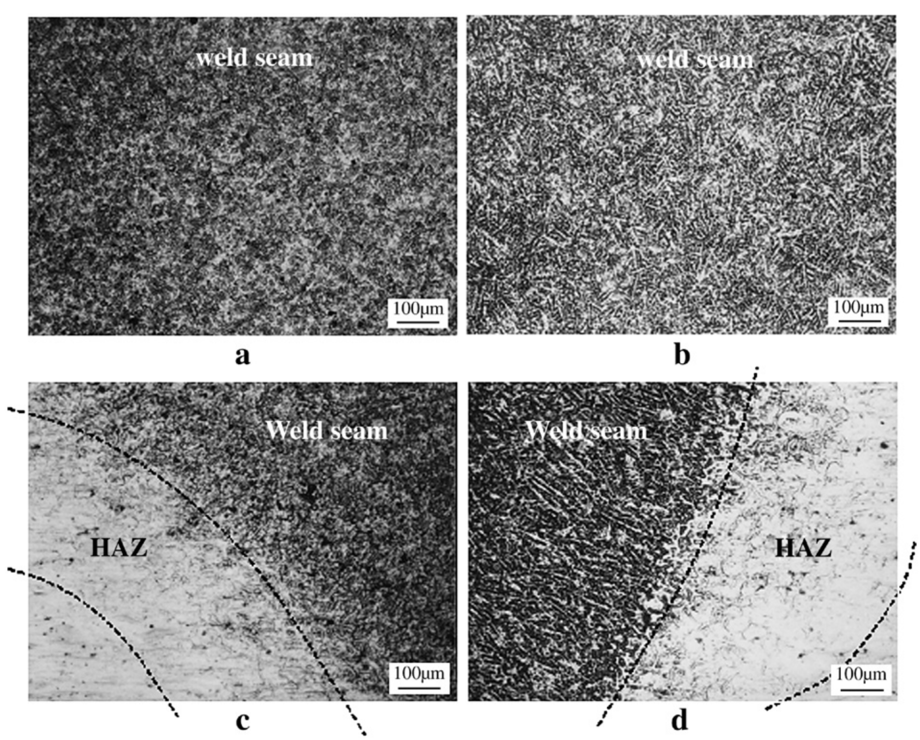

Fig. 4 – Optical macrostructure of GTA welded Mg-AZ31B alloy prepared without flux (a, c) and with a $CdCl_2$ flux (b,d).

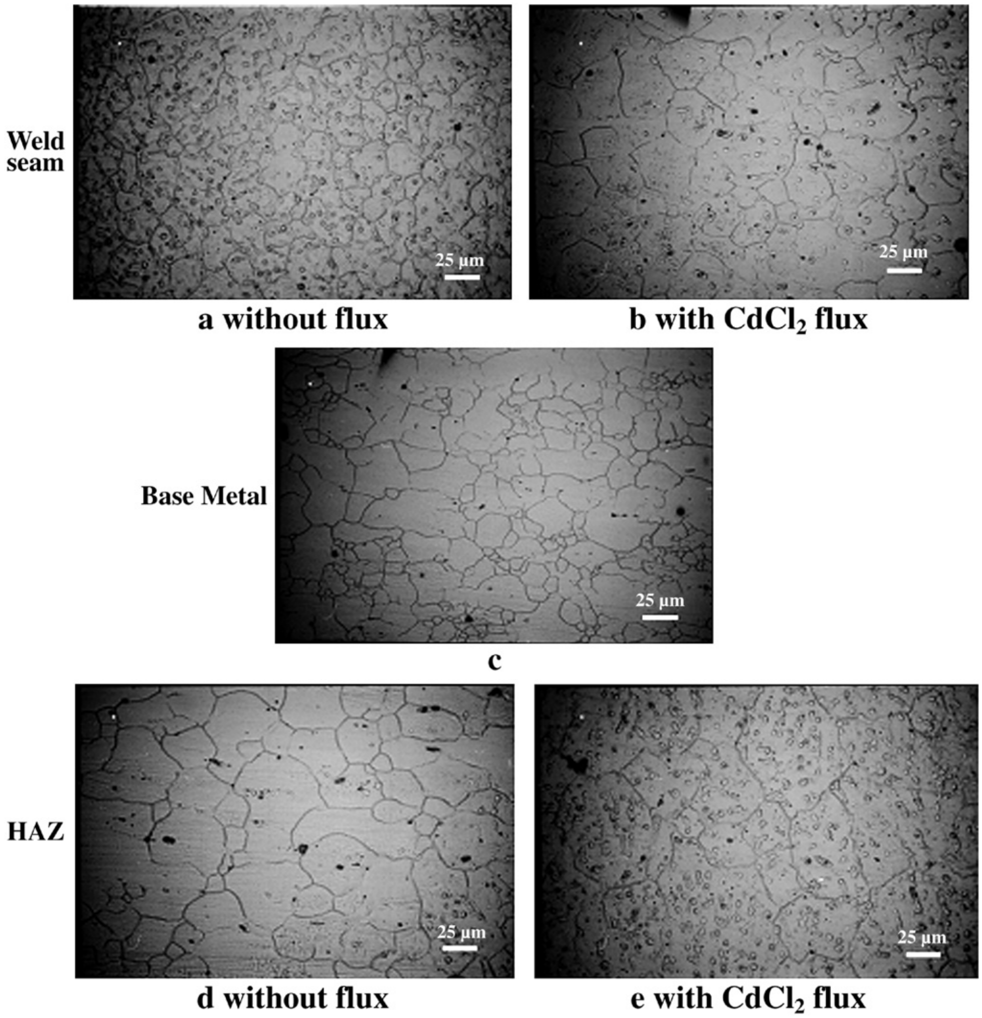

Fig. 5 – Optical macrostructure of GTA welded Mg-AZ31B alloy with and without $CdCl_2$ flux.

low melting temperature (≈450 °C) β-$Mg_{17}Al_{12}$ phase will form due to the eutectic reaction L→α-Mg+β-$Mg_{17}Al_{12}$. During the GTA welding process, the solidification process of the metal in the weld seam is a non-equilibrium process, and the β-$Mg_{17}Al_{12}$ could appear under the rapid cooling rate. Energy dispersive spectroscopy (EDS) indicated that the white dot regions contain up to 12.65 and 13.05 wt.% of Al and Zn, respectively, while the black pit contains 100 wt.% Mg. The black pits are presumably formed when the white dots are etched and pulled out of the surface; thus, the black pit regions are primarily the Mg alloy matrix. The white dot phase is predominantly comprised of Al and Zn, and was identified as the $Mg_{17}(Al,Zn)_{12}$ phase by X-ray diffraction, as shown in Fig. 7 [the Zn contribution is not indicated in the legend].

Fig. 8 shows high-magnification compositional maps from EPMA analyses of the weld seam of the GTA weld prepared with the $CdCl_2$ flux. The images in the lower right show back-scattered images of the microstructure over a 256 μm × 256 μm area. The other images show the elemental distributions for Mg, Al, Zn, Cd and Cl. In the compositional maps, bright colors indicate regions of high concentration. The back-scattered images show the presence of a second phase in the micro-structures; this is identified as the $Mg_{17}(Al,Zn)_{12}$ phase indicated by the optical micrographs in Figs. 6b and 7. In activated flux GTA welding, a thin layer of the flux is deposited on the surface of the joint before welding. During the welding process, the flux containing element may be transferred into the weld metal. Elements contained in the flux can change the temperature coefficient of the surface tension from negative to positive and further change the direction of the fluid flow in the weld pool. In that case, a relatively deep and narrow weld will be produced. In the present experiments, the distributions of cadmium, chlorine in the weld were measured with EPMA. The regions measured included the top, bottom and middle of the weld fusion zone, and the zone adjacent to the fusion boundary. Neither Cd nor Cl was found in the weld zone; results for the other zones were similar. The results shown in Fig. 8 are representative; the $CdCl_2$ flux has a small effect on convection in the weld pool.

3.3. *Tensile Properties*

The strength of the base material and the weld prepared with and without the $CdCl_2$ flux are shown in Fig. 9. These results show that: (i) the base material strength is considerably higher than that of the weld metals and HAZs, (ii) the strength of the

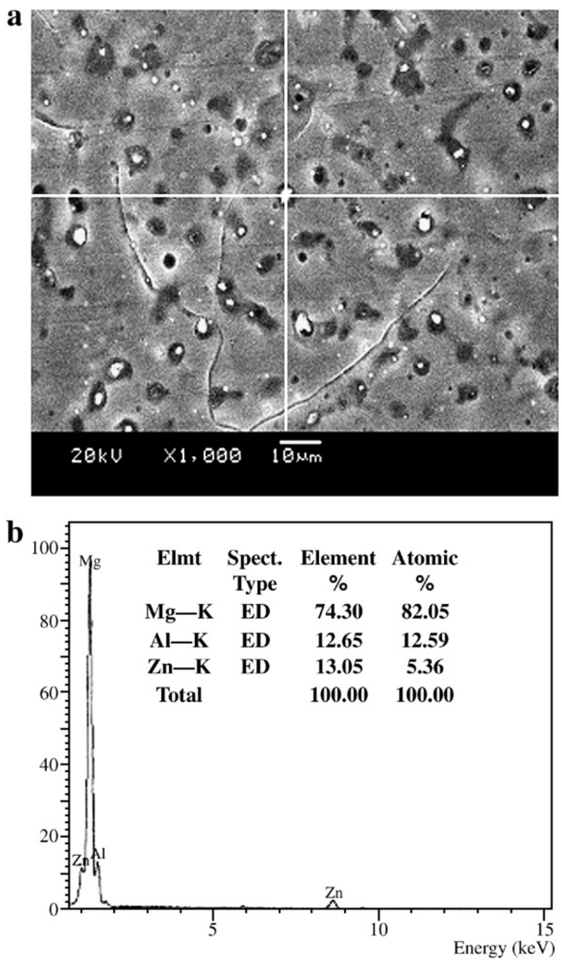

Fig. 6 – (a) Secondary electron images, and (b) EDS analysis fusion zone of the GTA weld prepared with a $CdCl_2$ flux.

weld metal prepared without the use of the flux are a little higher than that prepared with the $CdCl_2$ flux, and (iii) the L specimen tensile strength is a little higher than that of the T specimen.

The base metal used in our experiment is a wrought Mg alloy, in which the grain microstructure appears fibrous (see Fig. 5c). This means that the mechanical properties of base metal are orientation-dependent. The tensile strength of the rolling/parallel fiber (H specimen) is higher than that of the transverse/vertical fiber (V specimen). The wrought metal has higher properties than the as-cast metal because of this orientation strengthening effect. It can be seen in Fig. 9 that the tensile strength of the GTA welded joint without flux is about 94% of the base metal strength, and the tensile strength of the flux-welded joint is about 91% of the base metal strength. From the microstructure of the weld joints (Fig. 5), the grains in the fusion zone are relatively fine compared to the coarser grain size in the HAZ. In the tensile tests fracture always occurred in the HAZ zone, a relatively weak zone in welded joints of the Mg alloy. In the GTA weld prepared with $CdCl_2$ flux, the HAZ was slightly larger than that of the weld prepared without flux. This further decreased the tensile strength of the weld joint prepared with flux. Also, when the weld metal was located in the center of the gauge length (T specimen), the tensile strength was lower than that of the L specimen. This can also be explained based on microstructural refinement caused by the relatively high cooling rates that occur in the fusion zone and the microstructural coarsening that occurs in the HAZ.

3.4. *Hardness*

Particular attention was also given to weld metal mechanical properties by monitoring the hardness. The results of microhardness measurements in the weld fusion zone, the HAZ and the base material in as-weld specimens are shown in Fig. 10 (without flux) and Fig. 11 (with $CdCl_2$ flux). A hardness reduction in the weld metal and the HAZ compared with the base metal is evident. The base metal possessed a hardness that remained fairly constant around 62 Vickers. The microhardness of the weld metal shows some variability, and it appears that there is little change in the microhardness of the

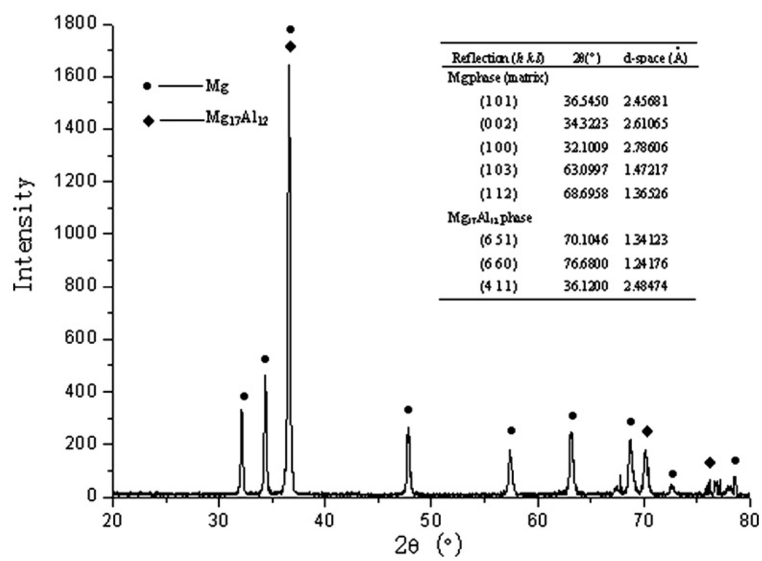

Fig. 7 – XRD analysis of the fusion zone of the GTA weld prepared with a $CdCl_2$ flux.

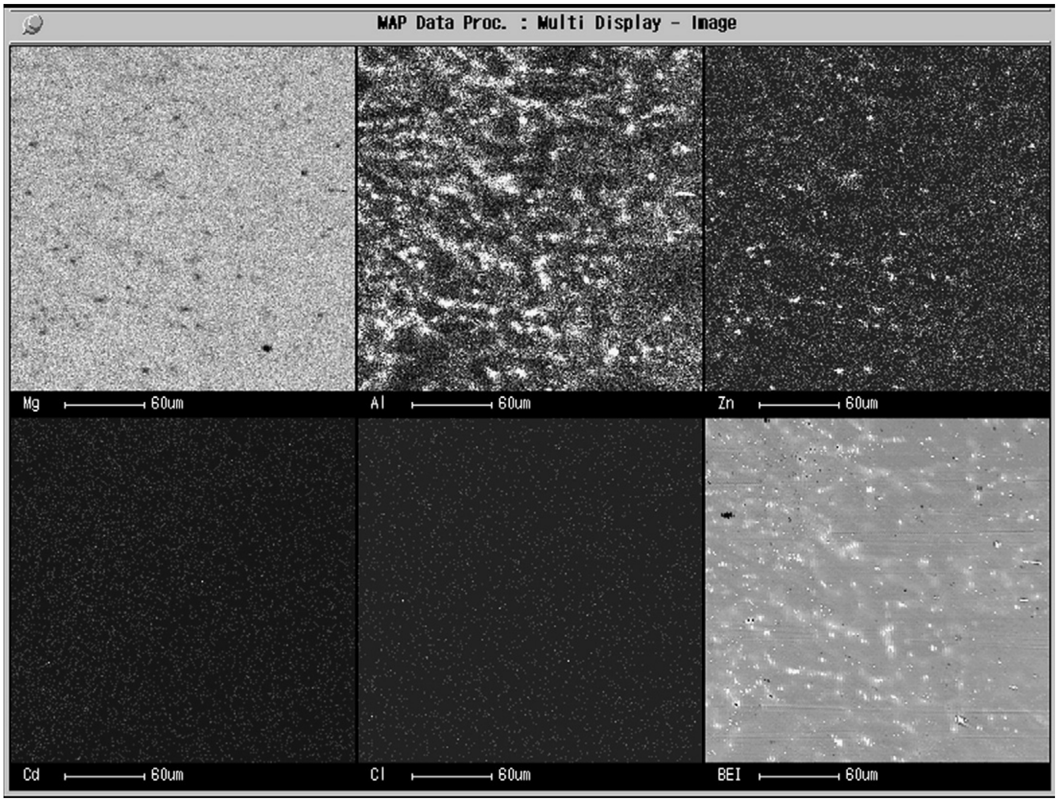

Fig. 8 – Back-scattered electron images and compositional maps in the weld seam of the GTA weld prepared with a $CdCl_2$ flux.

welded zone for the GTA welds prepared with and without flux.

4. Summary and Conclusions

Gas tungsten arc (GTA) welds were prepared on 5-mm thick plates of wrought magnesium AZ31B alloy, using an activated flux. The welds were subjected to a number of metallographic, tensile and microhardness examinations in order to determine differences in the welds prepared by the two different processes. This study yielded the following results:

- The weld penetration of the GTA weld prepared with a $CdCl_2$ flux is twice that for a weld prepared without flux. No defects were observed in either weld or their heat affected zones.
- Larger grain sizes were observed in the as-welded fusion zone prepared with a $CdCl_2$ flux; the HAZ was also slightly wider. These characteristics led to lower tensile strength compared to that of the welds prepared without the use of a flux.
- In the as-welded condition, the fusion zone microstructure consisted of matrix α-Mg, eutectic α-Mg and β-$Mg_{17}Al_{12}$, as identified by XRD, EDS and EPMA.
- Neither Cd nor Cl was detected in the weld seam by EPMA, indicating that the $CdCl_2$ flux has little effect on convection in the weld pool.
- The results of microhardness measurements shows a hardness reduction in the weld metal and HAZ as compared with the base metal is evident; however, there was little

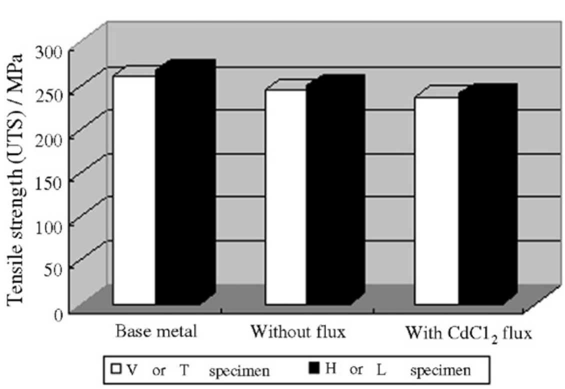

Fig. 9 – Room temperature tensile test results.

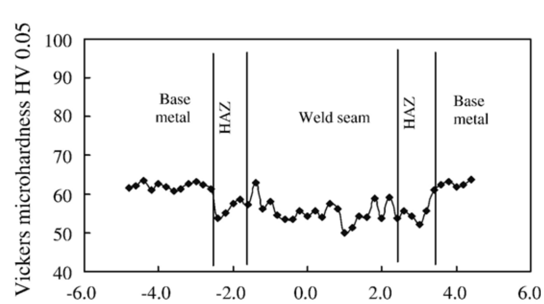

Fig. 10 – Microhardness of the weld joint prepared without flux.

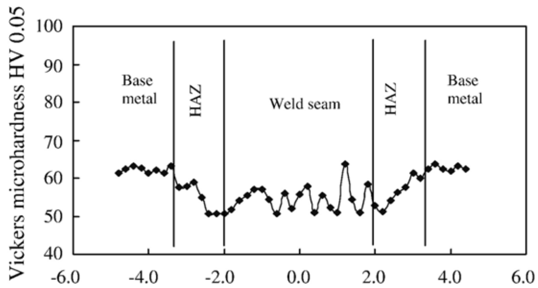

Fig. 11 – Microhardness of the weld joint prepared with a $CdCl_2$ flux.

difference in the microhardness of the GTA welds prepared with and without flux.

Acknowledgment

The authors gratefully acknowledge the sponsorship from Program for New Century Excellent Talents in University under project NCET-04-0271 and the Excellent Young Teachers Program of MOE, P. R. C.

REFERENCES

[1] Mordike BL, Ebert T. Magnesium properties–applications–potential. Mater Sci Eng A 2001;302:37–45.
[2] Roberts CS. Magnesium and Its Alloys. New York: John Wiley and Sons; 1960.
[3] Lee S, Lee SH, Kim DH. Effect of Y Sr and Nd additions on the microstructure and microfracture mechanism of squeeze-cast AZ91-X magnesium alloys. Metall Mater Trans A 1998;29:1221–35.
[4] Munitz A, Cotler C, Stern A, Kohn G. Mechanical properties and microstructure of gas tungsten arc welded magnesium AZ91D plates. Mater Sci Eng A 2001;302:68–73.
[5] Sun Z, Pan D. Comparative evaluation of tungsten inert gas and laser welding of AZ31 magnesium alloy. Sci Technol Weld Join 2002;7:343–51 [Wei J].
[6] Asahina T, Tokisue H. Electron bean weldability of pure magnesium and AZ31 magnesium alloy. Mater Trans 2001;42:2345–53.
[7] Liu LM, Wang JF, Gang S. Hybrid laser-TIG welding, laser beam welding and gas tungsten arc welding of AZ31B magnesium alloy. Mater Sci Eng A 2004;381:129–33.
[8] Song G, Liu L, Chi M, Wang JF. Investigations on laser-TIG hybrid welding of magnesium alloys. Mater Sci Forum 2005;488–489:371–5.
[9] Cao X, Jahazi M, Immarigeon JP, Wallace W. A review of laser welding techniques for magnesium alloys. J Mater Process Technol 2006;171:188–204.
[10] Zhu TP, Chen ZW, Gao W. Incipient melting in partially melted zone during arc welding of AZ91D magnesium alloy. Mater Sci Eng A 2006;416:246–52.
[11] Zhang ZD, Liu LM, Shen Y, Wang L. Welding of magnesium alloys with activating flux. Sci Technol Weld Join 2005;10:737–43.
[12] Liu LM, Zhang ZD, Song G, Shen Y. Effect of cadmium chloride flux in active flux TIG welding of magnesium alloys. Mater Trans 2006;74:446–9.
[13] Marya M. Theoretical and experimental assessment of chloride effects in the A-TIG welding of magnesium. Weld World 2002;46:7–21.
[14] Marya M, Edwards GR. Chloride contributions in flux-assisted GTA welding of magnesium alloys. Weld J 2002;81:291-s–8-s.
[15] Gurevich SM, Zamkov VN, Kushmienko NA. Improving the penetration of titanium alloys when they are welded by argon tungsten arc process. Avtom Svarka 1965;9:1–4.
[16] Gurevich SM, Zamkov VN. Welding titanium with a non-consumable electrode using fluxes. Avtom Svarka 1966;12:13–6.